

Selection of the optimal condition for the production of light neutron-rich isotopes in multinucleon transfer reactions

Shuqing Guo,^{1,2} Xiaojun Bao,³ and Nan Wang^{1,*}

¹*College of Physics and Energy, Shenzhen University, Shenzhen 518060, China*

²*Key Laboratory of Optoelectronic Devices and Systems of Ministry of Education and Guangdong Province, College of Optoelectronic Engineering, Shenzhen University, Shenzhen 518060, China*

³*Department of Physics, Hunan Normal University, Changsha 410081, China*



(Received 15 December 2020; accepted 8 March 2021; published 16 March 2021)

Light neutron-rich isotopes are populated as products of the multinucleon transfer reaction following the collisions of ^{64}Ni beams onto ^{130}Te , ^{208}Pb , and ^{238}U targets and ^{40}Ar beams onto ^{197}Au , ^{208}Pb , and ^{238}U targets at bombarding energies slightly above the Coulomb barrier. Distribution characteristics of projectile-like fragments are studied in the framework of dinuclear system concept where dynamic deformation is taken into account. The odd-even effect in the diffusion process is discussed, and the distribution of final isotopes can be well reproduced by the effective local excitation energies excluding pairing energies. Compared with the experimental data, it is found that the heavier (i.e., larger N/Z ratio) the target is, the more likely it is to produce light neutron-rich isotopes.

DOI: [10.1103/PhysRevC.103.034613](https://doi.org/10.1103/PhysRevC.103.034613)

I. INTRODUCTION

The nucleus is a finite quantum many-body system composed of fermions characterized by a shell structure in the single-particle spectra. Nuclei with some valence particles around the closed-shell closure provide an ideal laboratory environment for the understanding of nuclear structure and the effective nucleon-nucleon interaction [1]. In particular, with the production of nuclei far from the β -stability line, it is possible to explore the evolution of the known shell closures for large range of N/Z ratios and to characterize new regions of nuclear deformation [2,3]. However, most of these nuclei predicted to exist lack experimental data, especially those in the region of very neutron rich in the nuclide chart. There is no ideal way to fill this area and to reach the neutron drip line [4]. Since binary reactions between stable beams and heavy targets can produce moderately neutron-rich and neutron-deficient species and populate them to their high spin states, it is now feasible to investigate the production characteristics of these nuclei by multinucleon transfer (MNT) reactions [5,6], which also provide us with an opportunity to address the spectroscopy study of nuclei that cannot be accessed in other reactions [7–10].

The MNT reaction, in which many nucleons are transferred to (or from) the target nucleus, has been extensively studied in experiment over the last few decades [11]. In a recent review [12], experimental production cross sections for several nucleon transfers in $^{136}\text{Xe} + ^{198}\text{Pt}$ reaction are found to be relatively large. The renewed interest in MNT reaction at incident energies near the Coulomb barrier attracts great attention

to produce the new neutron-rich nuclei in both experimental [4,12–16] and theoretical studies [17–34]. The advantage of the MNT reaction becomes more and more striking when producing neutron-rich nuclei in the region of the neutron shell closure $N = 126$ [12]. Nevertheless, a basic problem of MNT reactions in producing heavy neutron-rich isotopes is that higher projectile energies can broaden the distribution range of isotopes but lead to fission of the heavy excited target-like fragments [14,35]. Consequently, most experimental studies of MNT reactions with actinide targets have been performed near or below the Coulomb barrier. In general, the experiments using MNT reactions are more likely to provide light neutron-rich projectile-like fragments and their detail spectra than fragmentation reactions or intermediate energy Coulomb excitation reactions [36]. In this respect, the recent experimental advances in MNT reactions allow us now to further investigate the production mechanism of very neutron-rich nuclei in the vicinity of the light partner.

Theoretical study on the mechanism of isotope production in MNT reactions is of great significance, where one of the most important purposes is to recommend optimal experimental conditions for the production of neutron-rich nuclei of interest. From the point of view of the experimental verification, the systematic calculation of the production distribution of neutron-rich projectile-like fragments are investigated. The main purpose of the present work is that the expected characteristics of production distribution can help evaluate the optimal conditions for producing light neutron-rich isotopes.

II. THEORETICAL FRAMEWORK

The production cross section of a primary product $\sigma_{Z_1, N_1}^{\text{pri}}(E_{\text{c.m.}})$ in the diffusive nucleon transfer reaction based on

* wangnan@szu.edu.cn

the present DNS model with dynamic deformation taken into account can be calculated by a sum over all partial waves J ,

$$\sigma_{Z_1, N_1}^{\text{pri}}(E_{\text{c.m.}}) = \frac{\pi \hbar^2}{2\mu E_{\text{c.m.}}} \sum_J (2J+1) T(E_{\text{c.m.}}, J) \times \sum_{\beta_1, \beta_2} P(Z_1, N_1, \beta_1, \beta_2, J, \tau_{\text{int}}), \quad (1)$$

where the penetration coefficient $T(E_{\text{c.m.}}, J)$ is estimated to be 1 when the incident energy is higher than the Coulomb barrier at the injection point. Since the Coulomb barrier of a sufficiently heavy system may disappear, the injection point where the nucleon transfer process takes places can be assumed by $R_{\text{cont}} = R_1[1 + \beta_1 Y_{20}(\theta_1)] + R_2[1 + \beta_2 Y_{20}(\theta_2)] + 0.5$ fm, with $R_i = 1.16A_i^{1/3}$ [37].

The multinucleon rearrangement process between the colliding projectile and target is described as a diffusion process. Meanwhile, the dynamic deformation is expected to be considered in the process from the contacting of the colliding nuclei to the separation of projectile-like and target-like products [37,38]. Combinations of the Coulomb, nuclear, and centrifugal potentials of various DNS configurations define a four macroscopic variables potential-energy surface, $U(Z_1, N_1, \beta_1, \beta_2)$, whose gradients drive the evolution of the reaction products during the collision. Probability of the distribution function $P(Z_1, N_1, \beta_1, \beta_2; t)$ to find fragment 1 with Z_1, N_1, β_1 and fragment 2 with Z_2, N_2, β_2 at time t is described by the following master equation [37]:

$$\begin{aligned} & \frac{dP(Z_1, N_1, \beta_1, \beta_2; t)}{dt} \\ &= \sum_{Z'_1} W_{Z_1, N_1, \beta_1, \beta_2; Z'_1}(t) [d_{Z_1, N_1, \beta_1, \beta_2} P(Z'_1, N_1, \beta_1, \beta_2; t) \\ & \quad - d_{Z'_1, N_1, \beta_1, \beta_2} P(Z_1, N_1, \beta_1, \beta_2; t)] \\ & \quad + \sum_{N'_1} W_{Z_1, N_1, \beta_1, \beta_2; N'_1}(t) [d_{Z_1, N_1, \beta_1, \beta_2} P(Z_1, N'_1, \beta_1, \beta_2; t) \\ & \quad - d_{Z_1, N'_1, \beta_1, \beta_2} P(Z_1, N_1, \beta_1, \beta_2; t)] \\ & \quad + \sum_{\beta'_1} W_{Z_1, N_1, \beta_1, \beta_2; \beta'_1}(t) [d_{Z_1, N_1, \beta_1, \beta_2} P(Z_1, N_1, \beta'_1, \beta_2; t) \\ & \quad - d_{Z_1, N_1, \beta'_1, \beta_2} P(Z_1, N_1, \beta_1, \beta_2; t)] \\ & \quad + \sum_{\beta'_2} W_{Z_1, N_1, \beta_1, \beta_2; \beta'_2}(t) [d_{Z_1, N_1, \beta_1, \beta_2} P(Z_1, N_1, \beta_1, \beta'_2; t) \\ & \quad - d_{Z_1, N_1, \beta_1, \beta'_2} P(Z_1, N_1, \beta_1, \beta_2; t)], \quad (2) \end{aligned}$$

where $W_{Z_1, N_1, \beta_1, \beta_2; Z'_1} \equiv W_{Z_1, N_1, \beta_1, \beta_2; Z'_1, N_1, \beta_1, \beta_2}$ is the mean transition probability from the macroscopic state $(Z'_1, N_1, \beta_1, \beta_2)$ to the macroscopic state $(Z_1, N_1, \beta_1, \beta_2)$. $d_{Z_1, N_1, \beta_1, \beta_2}$ denotes the number of microscopic states corresponding to the macroscopic state $(Z_1, N_1, \beta_1, \beta_2)$. The β_1 and β_2 which are considered as two discrete variables denote quadrupole deformations of projectile-like and target-like fragments, respectively. Only the tip-to-tip configuration is considered in present work. The initial condition of Eq. (2) is $P(Z_P, N_P, \beta_P, \beta_T; t=0) = 1$, with the Z_P, N_P, β_P , and β_T corresponding to the proton

and neutron number and the ground-state quadrupole deformations of projectile and target in the entrance channel. The interaction time τ_{int} in the dissipative process of two colliding nuclei is calculated by using the deflection function method [39–41]. The mean transition probability and the number of microscopic states are mainly determined by the local excitation energy and potential-energy surface. See Ref. [37] for more details.

To obtain the production cross section of the final isotopes $\sigma_{Z_1, N_1}^{\text{fin}}(E_{\text{c.m.}})$, the statistical model code GEMINI++ is employed, where subsequent deexcitation cascades of the excited initial fragments via the emission of light particles (neutron, proton, and α) and γ rays competing with the fission are taken into account [42–44]. The sharing of the total excitation energy between the primary projectile-like and the target-like fragments is assumed to be proportional to their masses. For a certain primary product, the deexcitation process should be simulated many times due to the statistical nature of GEMINI++. After M_{trial} times Monte Carlo simulations ($M_{\text{trial}} = 1000$ is adopted in present work), events with (Z_1, N_1) are counted, the number of such events is marked as $M(Z_1, N_1; Z'_1, N'_1, J')$. Then the decay probability from the primary product (Z'_1, N'_1, J') produced at the incident angular momentum J' to the final product (Z_1, N_1) can be estimated as $P(Z_1, N_1; Z'_1, N'_1, J') = M(Z_1, N_1; Z'_1, N'_1, J')/M_{\text{trial}}$. Finally, the production cross section of final product (Z_1, N_1) can be expressed as [29]

$$\sigma_{Z_1, N_1}^{\text{fin}}(E_{\text{c.m.}}) = \sum_{Z'_1, N'_1, J'} \sigma_{Z'_1, N'_1}^{\text{pri}}(E_{\text{c.m.}}, J') \times P(Z_1, N_1; Z'_1, N'_1, J'). \quad (3)$$

III. RESULTS AND DISCUSSIONS

To assess the ability of the present model in describing the MNT reaction, the production cross sections of projectile-like fragments in the collision of ^{64}Ni beams onto the respective ^{130}Te , ^{208}Pb , and ^{238}U targets at bombarding energies slightly above the corresponding Coulomb barriers are systematically calculated. Figure 1 shows the systematics of the production distribution of various projectile-like fragments in $^{64}\text{Ni} + ^{130}\text{Te}$ reaction at a bombardment energy of $E_{\text{c.m.}} = 184.27$ MeV. In each panel of the figure, the negative (or positive) number of transferred proton represents the number of proton removed from (or added to) the projectiles. For solid lines, they denote the calculated production cross sections of final projectile-like fragments by using the local excitation energy of the DNS configuration corrected by excluding the pairing energy, while for the dashed lines which have been calculated in recent work [45], such correction is not carried out. The experiment data are from the Ref. [36], as shown with symbols in Fig. 1. As can be seen from Fig. 1, there is a good overall agreement between experimental data and the results of the present work. However, if observed carefully, the calculated distributions of final projectile-like fragments without excluding the pairing energy from the local excitation energy are obviously staggering. On the one hand, the calculated isotopic distribution with the odd proton number are systematically lower than that with the neighboring even

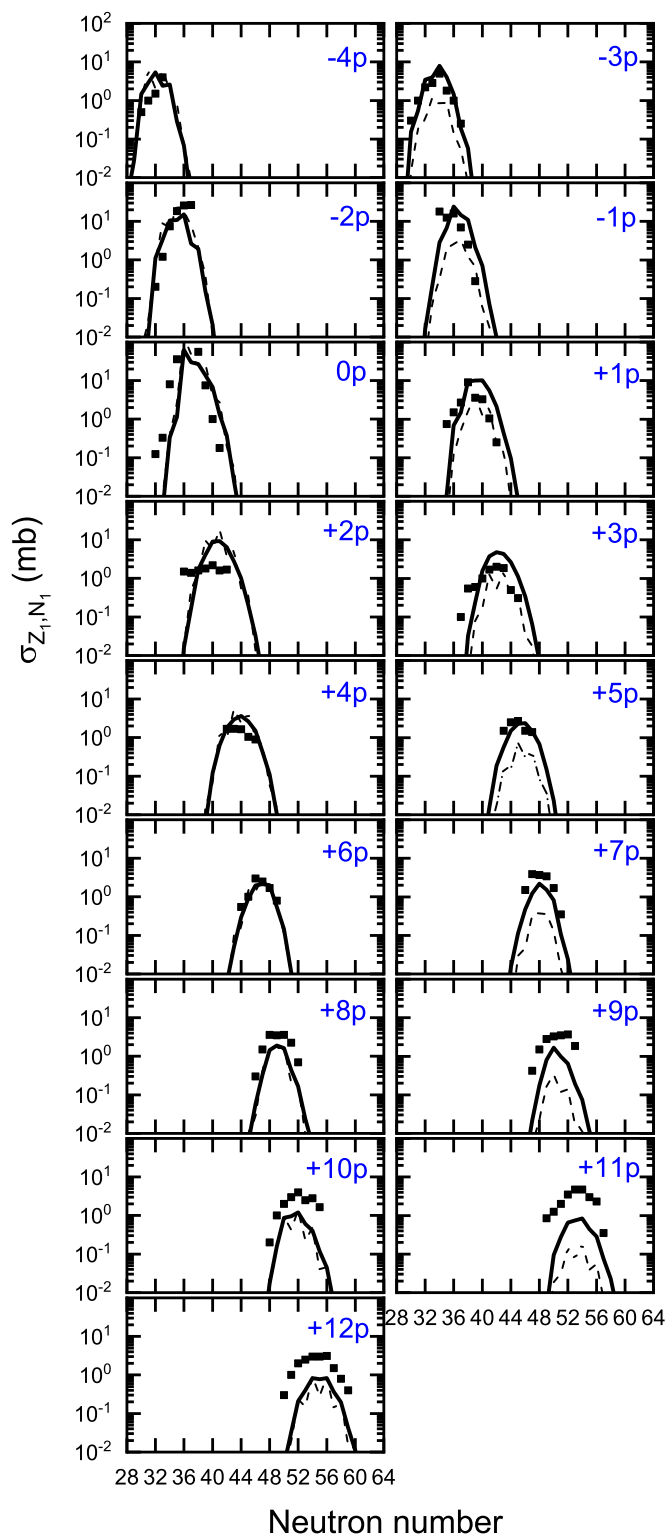


FIG. 1. Productions of projectile-like fragments in $^{64}\text{Ni} + ^{130}\text{Te}$ reaction at bombarding energy $E_{c.m.} = 184.27$ MeV. Solid (dashed) lines denote the calculations with (without) excluding the pairing energy in determining the local excitation energy. Measured cross sections are from Ref. [36].

proton number. On the other hand, variations of the distribution between excluding and not excluding the pairing energy are very significant in proton transfer channel with odd number, as shown in channel $-3p$, $-1p$, $+1p$, $+3p$, $+5p$, $+7p$, $+9p$, $+11p$, and $+13p$, respectively, while for the even- Z isotopic distribution, these variations are not obvious.

It is worth noting that the mentioned phenomena are not observed in experiment. The reason resulting in such variations of the calculation could be that the binding energy of one participant contains the pairing energy in the calculation of potential-energy surface of the DNS configuration [46], leading to the odd-even change of local excitation energy. As the underlying idea that the paired nucleons must be separated before each component can be excited individually, the corresponding pairing energy should be excluded for calculating the level density or the state density in many Fermi-gas type models [47]. That is the reason in present work for considering the excluding the pairing energy from the local excitation to calculate the microscopic number (or state density) of each DNS configuration. From this point of view, one should exclude the pairing energy when determining the effective local excitation, so that the calculated isotopic distributions do not exhibit any large odd-even staggering in almost all cases and reproduced the experiment excellently, as shown in Fig. 1 with solid lines.

The good ability of reproducing the experiment in the above $^{64}\text{Ni} + ^{130}\text{Te}$ reaction make us more confident to carry out more systematic research, such as the effect of different targets on the production distribution of projectile-like fragments. It should be emphasized that our studies are performed with one set of parameters and with the same assumptions for all investigations. To analyze the behavior of the same projectile ^{64}Ni bombarding different targets through MNT reaction, the production cross sections of projectile-like fragments in collision of $^{64}\text{Ni} + ^{208}\text{Pb}$ at $E_{c.m.} = 267.64$ MeV and $^{64}\text{Ni} + ^{238}\text{U}$ at $E_{c.m.} = 307.40$ MeV are calculated, as displayed in Figs. 2 and 3, respectively. It can be seen that the mentioned two MNT reactions are also well reproduced, sharing the similar distribution characteristics with the former one.

For the cases in the lighter area of the nuclide chart, we calculate the production cross sections of projectile-like fragments around the projectile ^{40}Ar in $^{40}\text{Ar} + ^{197}\text{Au}$ reaction at $E_{c.m.} = 180.37$ MeV, in $^{40}\text{Ar} + ^{208}\text{Pb}$ reactions at $E_{c.m.} = 214.70$ MeV and in $^{40}\text{Ar} + ^{238}\text{U}$ reactions at $E_{c.m.} = 226.87$ MeV. The comparison of the experimental data with the calculated cross sections of final projectile-like fragments are displayed in Figs. 4–6. Again the distributions of projectile-like fragments on the aspects of not only the trends but also the magnitudes are well reproduced. From Fig. 6, it can be found that the channel $-6p$ in the $^{40}\text{Ar} + ^{238}\text{U}$ reaction still has some odd-even change. This may due to the case that, for the very light fragments, their shared excitation energies caused by collisions slightly above the barrier may not be very large, so only a small amount of neutrons can be evaporated in the process of deexcitation. When the average number of evaporated neutrons is less than a unit, large statistical differences may be brought in.

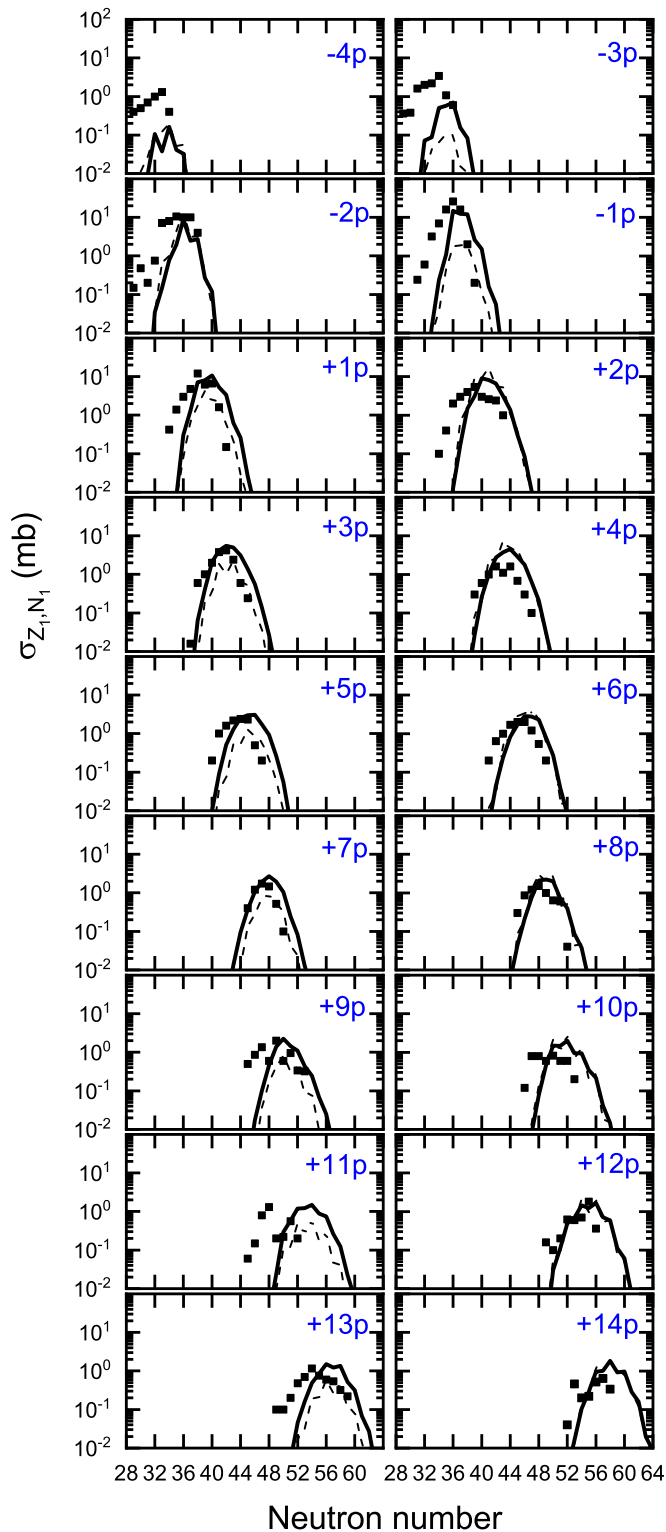


FIG. 2. Same as the Fig. 1, but for the $^{64}\text{Ni} + ^{208}\text{Pb}$ reaction at bombarding energy $E_{c.m.} = 267.64$ MeV. Measured cross sections are from Ref. [48].

It should be noted that the main purpose of our estimates of absolute cross sections is to provide useful guidelines to assess the optimal conditions for the production of light neutron-rich isotopes. For evaluating the isotopic distribution of selected

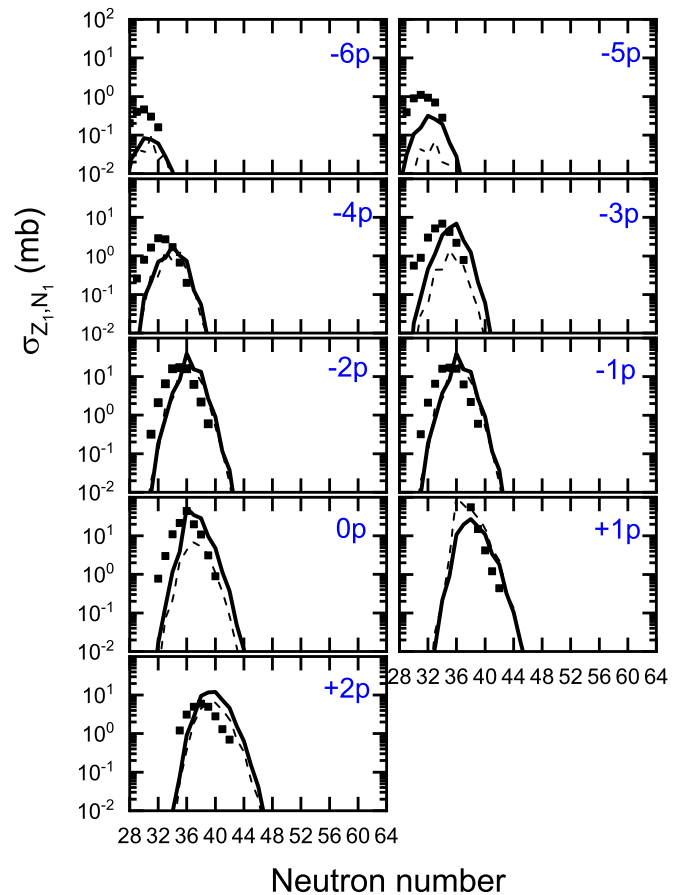


FIG. 3. Same as the Fig. 1, but for the $^{64}\text{Ni} + ^{238}\text{U}$ reaction at bombarding energy $E_{c.m.} = 307.40$ MeV. Measured cross sections are from Ref. [49].

elements, we compared the cross sections of specific isotopes obtained by different target-based collisions with corresponding experimental results. Figure 7 shows a comparison of the final isotopic distributions of the projectile-like fragments in reactions of $^{64}\text{Ni} + ^{130}\text{Te}$, ^{208}Pb , and ^{238}U . Here take the Fe ($-2p$ channel) isotopic distribution for example, which are formed by transferring two protons and various neutrons from projectile to target. As can be seen from the figure, the distribution of the transfer cross sections is very narrow, but the neutron-rich Fe isotopes from $A = 62$ to 66 have competitive formations at the microbarn level, which can be studied by selective gamma coincidence analysis [36]. The production of neutron-rich isotopes observed in the $^{64}\text{Ni} + ^{238}\text{U}$ reaction, as shown in Fig. 7 is one to two orders of magnitude higher than that of the other two reactions, especially in the case of very-rich-neutron regions, indicating that heavier targets are quite encouraging for production of light neutron-rich nuclei. The explanation could be that because the N/Z value of the populated fragments naturally come close to that of the composite system, the more intense flow of protons from the small N/Z valued projectile ^{64}Ni (1.286) to the large N/Z valued target ^{130}Te (1.500), ^{208}Pb (1.537), or ^{238}U (1.587) can populate target-like fragments with higher Z and projectile-like fragments with lower Z . It is worth noting that the use of the

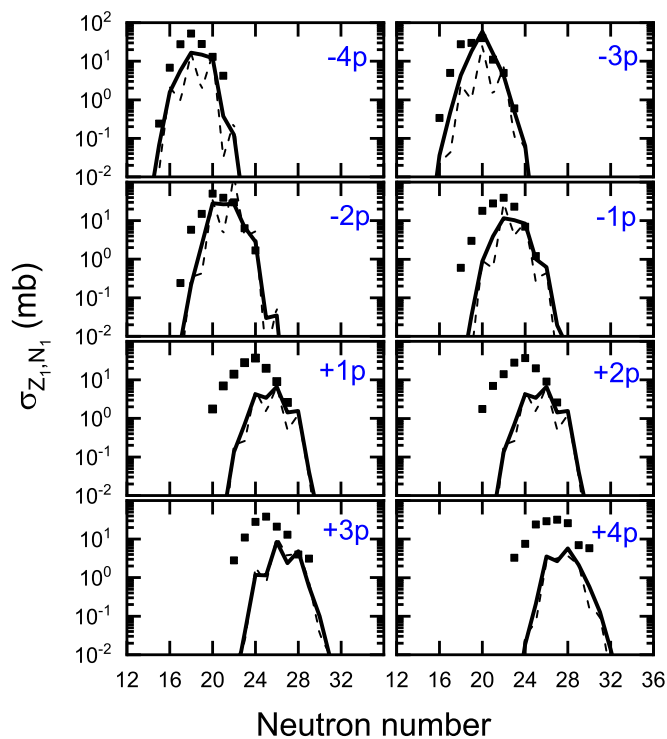


FIG. 4. Same as the Fig. 1, but for the $^{40}\text{Ar} + ^{197}\text{Au}$ reaction at bombarding energy $E_{c.m.} = 180.37$ MeV. Measured cross sections are from Ref. [50].

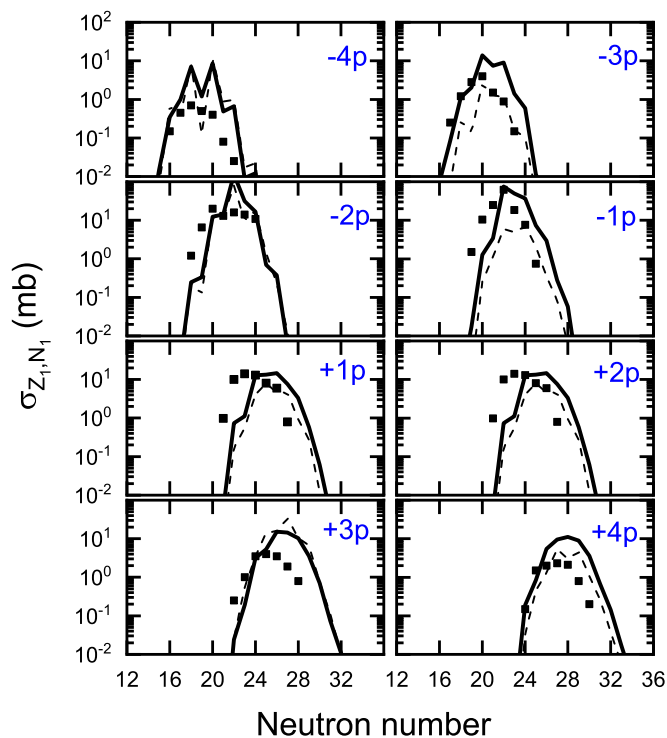


FIG. 5. Same as the Fig. 1, but for the $^{40}\text{Ar} + ^{208}\text{Pb}$ reaction at bombarding energy $E_{c.m.} = 214.70$ MeV. Measured cross sections are from Ref. [51].

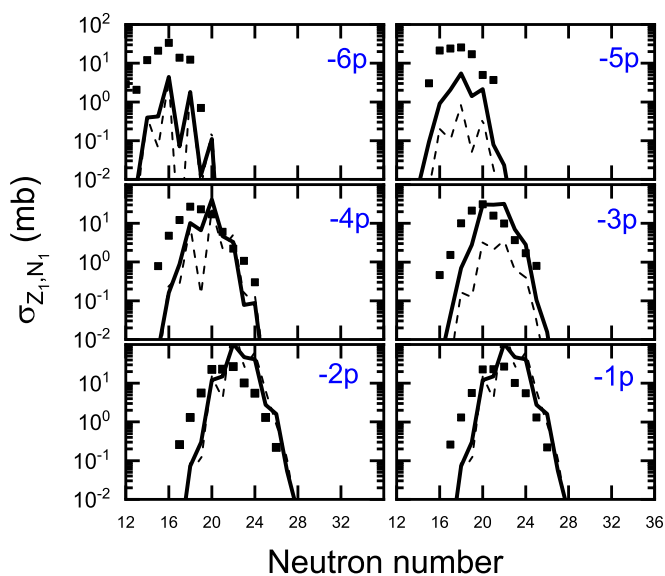


FIG. 6. Same as the Fig. 1, but for the $^{40}\text{Ar} + ^{238}\text{U}$ reaction at bombarding energy $E_{c.m.} = 226.87$ MeV. Measured cross sections are from Ref. [50].

^{238}U target with the largest N/Z value provides the best way to study neutron-rich nuclei located in the vicinity of projectile. Similar behavior, in the systems $^{40}\text{Ar} + ^{179}\text{Au}$, $^{40}\text{Ar} + ^{208}\text{Pb}$, and $^{40}\text{Ar} + ^{238}\text{U}$, also can be found in Fig. 8. At first glance, in Figs. 7(a) and 8(a), most of the experimental data are quite overlapped near the peak position of isotopic distribution, but for the neutron-rich isotopes relatively far from the peak position, the advantage of heavier (i.e., larger N/Z ratio) targets to produce very neutron-rich (light) isotopes becomes

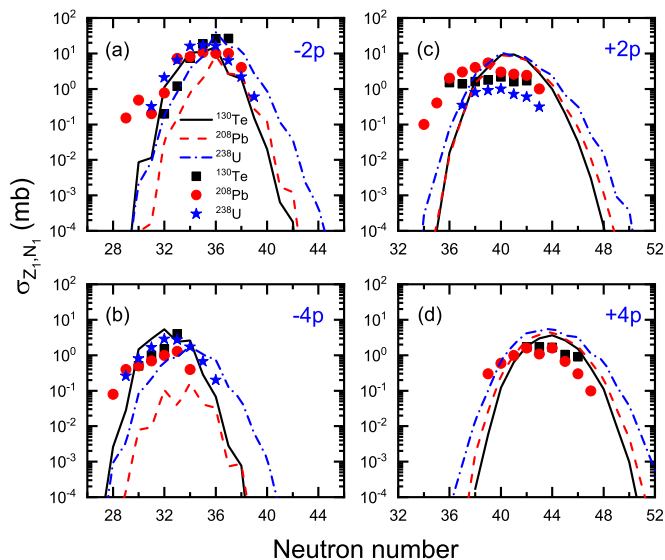


FIG. 7. The comparison of production cross sections of projectile-like fragments in MNT reactions with the beam ^{64}Ni bombarding the targets ^{130}Te , ^{208}Pb , and ^{238}U at $E_{c.m.} = 187.27$, 267.64 , and 307.40 MeV, respectively. Measured cross sections are from Refs. [36,48,49].

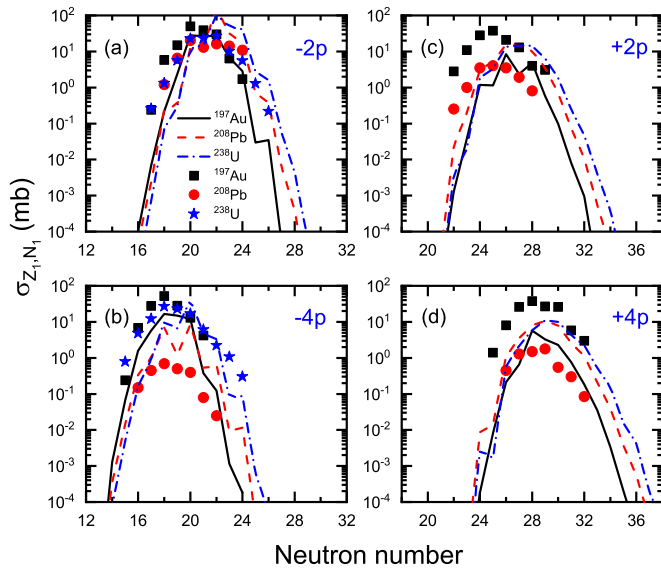


FIG. 8. The comparison of production cross sections of projectile-like fragments in MNT reactions with the beam ^{40}Ar bombarding the targets ^{197}Au , ^{208}Pb , and ^{238}U at $E_{\text{c.m.}} = 180.37, 214.70,$ and 226.87 MeV, respectively. Measured cross sections are from Refs. [50,51].

obvious. For the large deviation of Pb with experimental data, especially in Figs. 8(c) and 8(d), we propose a rather simple explanation. On the one hand, the inflexible Pb target corresponds to a higher barrier, thus the lower local excitation near the incident channel caused by near barrier collision may result in the slower diffusion rate and the smaller transfer cross section, while for the calculation in present work, employed barrier distribution will increase the local excitation energy

and thus overestimate the experimental results. On the other hand, as stated in the experimental reference, the detection angle is quite close to the grazing angle, so it is difficult to distinguish the quasi-elastic collision from the deep-inelastic component. The conclusion drawn from the systematic trend of calculation and the comparison with experiment shows that the heavier targets with larger N/Z ratio are preferable for the production of light neutron-rich nuclei.

IV. SUMMARY

The distribution characteristics of projectile-like fragments have been studied in reactions of $^{64}\text{Ni} + ^{130}\text{Te}$, ^{208}Pb , and ^{238}U , and $^{40}\text{Ar} + ^{197}\text{Au}$, ^{208}Pb , and ^{238}U with bombarding energies slightly above the Coulomb barriers. Experimental production cross section of projectile-like isotopes are well reproduced with the consideration of dynamic deformation. Taking into account the effect of pair breaking of neutron and proton in transfer process, the effective local excitation energies of various DNS configurations are corrected by excluding the corresponding pairing energies which can well describe the observed smooth distribution of the isotopes. Systematic calculations show that the heavier (i.e., larger N/Z ratio) target is, the more likely it is to produce light neutron-rich isotopes. Such behavior could indicate again that MNT reaction can be used as a competitive tool for the production of neutron-rich nuclei in the vicinity of a light partner.

ACKNOWLEDGMENTS

The work was supported by the Natural Science Foundation of China (Grants No. 11847235, No. 11475115, and No. 11705118).

- [1] B. Brown, The nuclear shell model towards the drip lines, *Prog. Part. Nucl. Phys.* **47**, 517 (2001).
- [2] J. Prisciandaro, P. Mantica, B. Brown *et al.*, New evidence for a subshell gap at $N = 32$, *Phys. Lett. B* **510**, 17 (2001).
- [3] T. Otsuka, R. Fujimoto, Y. Utsuno, B. A. Brown, M. Honma, and T. Mizusaki, Magic Numbers in Exotic Nuclei and Spin-Isospin Properties of the NV Interaction, *Phys. Rev. Lett.* **87**, 082502 (2001).
- [4] E. M. Kozulin, E. Vardaci, G. N. Knyazheva *et al.*, Mass distributions of the system $^{136}\text{Xe} + ^{208}\text{Pb}$ at laboratory energies around the Coulomb barrier: A candidate reaction for the production of neutron-rich nuclei at $N = 126$, *Phys. Rev. C* **86**, 044611 (2012).
- [5] W. von Oertzen and A. Vitturi, Pairing correlations of nucleons and multi-nucleon transfer between heavy nuclei, *Rep. Prog. Phys.* **64**, 1247 (2001).
- [6] L. Corradi, G. Pollarolo, and S. Szilner, Multinucleon transfer processes in heavy-ion reactions, *J. Phys. G* **36**, 113101 (2009).
- [7] H. Takai, C. N. Knott, D. F. Winchell *et al.*, Population of high spin states by quasi-elastic and deep inelastic collisions, *Phys. Rev. C* **38**, 1247 (1988).
- [8] S. Lunardi, S. M. Lenzi, F. Della Vedova, E. Farnea, A. Gadea, N. Mărginean *et al.*, Spectroscopy of neutron-rich Fe isotopes populated in the $^{64}\text{Ni} + ^{238}\text{U}$ reaction, *Phys. Rev. C* **76**, 034303 (2007).
- [9] S. Szilner, L. Corradi, F. Haas, D. Lehbertz, G. Pollarolo, C. A. Ur *et al.*, Interplay between single-particle and collective excitations in argon isotopes populated by transfer reactions, *Phys. Rev. C* **84**, 014325 (2011).
- [10] J. J. Valiente-Dobón, D. Mengoni, A. Gadea, E. Farnea, S. M. Lenzi, S. Lunardi *et al.*, Lifetime Measurements of the Neutron-Rich $N = 30$ Isotones ^{50}Ca and ^{51}Sc : Orbital Dependence of Effective Charges in the fp Shell, *Phys. Rev. Lett.* **102**, 242502 (2009).
- [11] P. Siemens, J. Bondorf, D. Gross, and F. Dickmann, Q -value dependence of heavy-ion transfer reactions above the Coulomb barrier, *Phys. Lett. B* **36**, 24 (1971).
- [12] Y. X. Watanabe, Y. H. Kim, S. C. Jeong, Y. Hirayama, N. Imai, H. Ishiyama *et al.*, Pathway for the Production of Neutron-Rich Isotopes Around the $N = 126$ Shell Closure, *Phys. Rev. Lett.* **115**, 172503 (2015).
- [13] D. Montanari, L. Corradi, S. Szilner, G. Pollarolo, E. Fioretto, G. Montagnoli *et al.*, Neutron Pair Transfer in $^{60}\text{Ni} + ^{116}\text{Sn}$ Far Below the Coulomb Barrier, *Phys. Rev. Lett.* **113**, 052501 (2014).
- [14] J. S. Barrett, W. Loveland, R. Yanez, S. Zhu, A. D. Ayangeakaa, M. P. Carpenter *et al.*, $^{136}\text{Xe} + ^{208}\text{Pb}$ reaction: A test of models

- of multinucleon transfer reactions, *Phys. Rev. C* **91**, 064615 (2015).
- [15] E. M. Kozulin, V. I. Zagrebaev, G. N. Knyazheva *et al.*, Inverse quasifission in the reactions $^{156,160}\text{Gd} + ^{186}\text{W}$, *Phys. Rev. C* **96**, 064621 (2017).
- [16] A. Vogt, B. Birkenbach, P. Reiter *et al.*, Light and heavy transfer products in $^{136}\text{Xe} + ^{238}\text{U}$ multinucleon transfer reactions, *Phys. Rev. C* **92**, 024619 (2015).
- [17] A. Winther, Grazing reactions in collisions between heavy nuclei, *Nucl. Phys. A* **572**, 191 (1994).
- [18] V. Zagrebaev and W. Greiner, Production of New Heavy Isotopes in Low-Energy Multinucleon Transfer Reactions, *Phys. Rev. Lett.* **101**, 122701 (2008).
- [19] V. I. Zagrebaev and W. Greiner, Production of heavy trans-target nuclei in multinucleon transfer reactions, *Phys. Rev. C* **87**, 034608 (2013).
- [20] G. G. Adamian, N. V. Antonenko, V. V. Sargsyan, and W. Scheid, Possibility of production of neutron-rich Zn and Ge isotopes in multinucleon transfer reactions at low energies, *Phys. Rev. C* **81**, 024604 (2010).
- [21] A. V. Karpov and V. V. Saiko, Modeling near-barrier collisions of heavy ions based on a Langevin-type approach, *Phys. Rev. C* **96**, 024618 (2017).
- [22] V. V. Saiko and A. V. Karpov, Analysis of multinucleon transfer reactions with spherical and statically deformed nuclei using a Langevin-type approach, *Phys. Rev. C* **99**, 014613 (2019).
- [23] A. Diaz-Torres, G. G. Adamian, N. V. Antonenko *et al.*, Melting or nucleon transfer in fusion of heavy nuclei? *Phys. Lett. B* **481**, 228 (2000).
- [24] Z. Q. Feng, Production of neutron-rich isotopes around $N = 126$ in multinucleon transfer reactions, *Phys. Rev. C* **95**, 024615 (2017).
- [25] L. Zhu, J. Su, W. J. Xie *et al.*, Theoretical study on production of heavy neutron-rich isotopes around the $N = 126$ shell closure in radioactive beam induced transfer reactions, *Phys. Lett. B* **767**, 437 (2017).
- [26] X. J. Bao, S. Q. Guo, J. Q. Li *et al.*, Influence of neutron excess of projectile on multinucleon transfer reactions, *Phys. Lett. B* **785**, 221 (2018).
- [27] S. Szilner, L. Corradi, G. Pollarolo *et al.*, Multinucleon transfer processes in $^{40}\text{Ca} + ^{208}\text{Pb}$, *Phys. Rev. C* **71**, 044610 (2005).
- [28] K. Sekizawa and K. Yabana, Time-dependent Hartree-Fock calculations for multinucleon transfer and quasifission processes in the $^{64}\text{Ni} + ^{238}\text{U}$ reaction, *Phys. Rev. C* **93**, 054616 (2016).
- [29] X. Jiang and N. Wang, Production mechanism of neutron-rich nuclei around $N = 126$ in the multi-nucleon transfer reaction $^{132}\text{Sn} + ^{208}\text{Pb}$, *Chin. Phys. C* **42**, 104105 (2018).
- [30] Z. Wu and L. Guo, Microscopic studies of production cross sections in multinucleon transfer reaction $^{58}\text{Ni} + ^{124}\text{Sn}$, *Phys. Rev. C* **100**, 014612 (2019).
- [31] N. Wang and L. Guo, New neutron-rich isotope production in $^{154}\text{Sm} + ^{160}\text{Gd}$, *Phys. Lett. B* **760**, 236 (2016).
- [32] C. Li, P. Wen, J. Li *et al.*, Production mechanism of new neutron-rich heavy nuclei in the $^{136}\text{Xe} + ^{198}\text{Pt}$ reaction, *Phys. Lett. B* **776**, 278 (2018).
- [33] C. Li, J. Tian, and F.-S. Zhang, Production mechanism of the neutron-rich nuclei in multinucleon transfer reactions: A reaction time scale analysis in energy dissipation process, *Phys. Lett. B* **809**, 135697 (2020).
- [34] F.-S. Zhang, C. Li, L. Zhu *et al.*, Production cross sections for exotic nuclei with multinucleon transfer reactions, *Front. Phys.* **13**, 132113 (2018).
- [35] J. Kratz, W. Loveland, and K. Moody, Syntheses of transuranium isotopes with atomic numbers $Z = 103$ in multi-nucleon transfer reactions, *Nucl. Phys. A* **944**, 117 (2015).
- [36] W. Królas, R. Broda, B. Fornal *et al.*, Dynamical deformation of nuclei in deep-inelastic collisions: A gamma coincidence study of $^{130}\text{Te} + 275\text{ MeV } ^{64}\text{Ni}$ and $^{208}\text{Pb} + 345\text{ MeV } ^{58}\text{Ni}$ heavy ion reactions, *Nucl. Phys. A* **832**, 170 (2010).
- [37] S. Q. Guo, X. J. Bao, H. F. Zhang, J. Q. Li, and N. Wang, Effect of dynamical deformation on the production distribution in multinucleon transfer reactions, *Phys. Rev. C* **100**, 054616 (2019).
- [38] S. Q. Guo, Y. Gao, J. Q. Li, and H. F. Zhang, Dynamical deformation in heavy ion reactions and the characteristics of quasifission products, *Phys. Rev. C* **96**, 044622 (2017).
- [39] G. Wolschin and W. Nörenberg, Analysis of relaxation phenomena in heavy-ion collisions, *Z. Phys. A: At. Nucl.* (1975) **284**, 209 (1978).
- [40] C. Riedel, G. Wolschin, and W. Nörenberg, Relaxation times in dissipative heavy-ion collisions, *Z. Phys. A: At. Nucl.* (1975) **290**, 47 (1979).
- [41] J. Q. Li and G. Wolschin, Distribution of the dissipated angular momentum in heavy-ion collisions, *Phys. Rev. C* **27**, 590 (1983).
- [42] R. J. Charity, Systematic description of evaporation spectra for light and heavy compound nuclei, *Phys. Rev. C* **82**, 014610 (2010).
- [43] D. Mancusi, R. J. Charity, and J. Cugnon, Unified description of fission in fusion and spallation reactions, *Phys. Rev. C* **82**, 044610 (2010).
- [44] <http://bitbucket.org/arekfu/gemini/src/master/>.
- [45] X. J. Bao, Role of neutron excess in the projectile for the production of heavy neutron-rich nuclei, *Phys. Rev. C* **102**, 054613 (2020).
- [46] N. Wang, M. Liu, and X. Wu, Modification of nuclear mass formula by considering isospin effects, *Phys. Rev. C* **81**, 044322 (2010).
- [47] T. Rauscher, F.-K. Thielemann, and K.-L. Kratz, Nuclear level density and the determination of thermonuclear rates for astrophysics, *Phys. Rev. C* **56**, 1613 (1997).
- [48] W. Krolas, R. Broda, B. Fornal *et al.*, Gamma coincidence study of $^{208}\text{Pb} + 350\text{ MeV } ^{64}\text{Ni}$ collisions, *Nucl. Phys. A* **724**, 289 (2003).
- [49] L. Corradi, A. M. Stefanini, C. J. Lin, S. Beghini, G. Montagnoli, F. Scarlassara, G. Pollarolo, and A. Winther, Multinucleon transfer processes in $^{64}\text{Ni} + ^{238}\text{U}$, *Phys. Rev. C* **59**, 261 (1999).
- [50] T. H. Chiang, D. Guerreau, P. Auger, J. Galin, B. Gatty, X. Tarrago, and J. Girard, Isotopic distributions in deep inelastic reactions induced by heavy ions and the relaxation of the neutron excess degree of freedom, *Phys. Rev. C* **20**, 1408 (1979).
- [51] T. Mijatović, S. Szilner, L. Corradi, D. Montanari, G. Pollarolo, E. Fioretto *et al.*, Multinucleon transfer reactions in the $^{40}\text{Ar} + ^{208}\text{Pb}$ system, *Phys. Rev. C* **94**, 064616 (2016).